Eur. Phys. J. A **27**, 77–90 (2006)
DOI 10.1140/epja/i2005-10229-5

THE EUROPEAN PHYSICAL JOURNAL A

Pion mass dependence of the nucleon mass in the chiral quark soliton model

K. Goeke[1], J. Ossmann[1], P. Schweitzer[1,a], and A. Silva[2]

[1] Institut für Theoretische Physik II, Ruhr-Universität Bochum, D-44789 Bochum, Germany
[2] Departamento de Física and Centro de Física Computacional, Universidade de Coimbra, P-3000 Coimbra, Portugal

Received: 25 May 2005 / Revised version: 21 December 2005 /
Published online: 20 February 2006 –
Communicated by U.-G. Meißner

Abstract. The dependence of the nucleon mass on the mass of the pion is studied in the framework of the chiral quark-soliton model. A remarkable agreement is observed with lattice data from recent full dynamical simulations. The possibility and limitations to use the results from the chiral quark soliton model as a guideline for the chiral extrapolation of lattice data are discussed.

PACS. 12.39.Fe Chiral Lagrangians – 11.15.Pg Expansions for large numbers of components (*e.g.*, $1/N_c$ expansions) – 12.38.Gc Lattice QCD calculations – 14.20.Dh Protons and neutrons

1 Introduction

The formulation of QCD on a discrete, finite Euclidean lattice [1] is at present the only strict and model-independent approach allowing to solve QCD in the low-energy regime and to study, *e.g.*, the hadronic spectrum from first principles [2]. Numerical lattice QCD simulations face technical problems, such as discretization errors or finite-size effects, which are attacked and minimized with increasing success by employing improved versions of discretized actions, or by working on larger lattices available thanks to the steadily growing computer power. Still, present lattices are too small to accommodate the pion as light as it appears in nature [3–11].

The tool needed to extrapolate lattice data from the region of nowadays typically $m_\pi \gtrsim 400\,\mathrm{MeV}$ down to the physical value of the pion mass is, in principle, provided by the chiral perturbation theory (χPT). The χPT is an effective but rigorous approach to the description of low-energy phenomena of strong interactions [12–14]. It is based on the concept of spontaneous chiral symmetry breaking with the pion as the Goldstone boson which acquires a small mass only due to explicit chiral symmetry breaking by the small current masses of the light quarks. χPT allows to address such questions like, *e.g.*, how much do baryon masses change if one "switches" on the masses of light quarks and varies their values.

In order to extrapolate reliably lattice data by means of χPT it is important to ensure the convergence of the chiral expansion up to large values of m_π. A first and promising *matching* of χPT and lattice results was reported, and it was established that the chiral expansion is well under control up to $m_\pi^2 < 0.4\,\mathrm{GeV}^2$ [15–18], see also [7]. More conservative estimates, however, indicate that the chiral expansion is reliable only up to $m_\pi^2 < 0.1\,\mathrm{GeV}^2$ [19]. The progress in computing power promises future lattice data at still lower pion masses and eventually at the physical point, which will improve the situation and make disappear this problem. In the meantime, however, it would be desirable to have a description of an intermediate region of pion masses, that would provide a safe *overlap* between the regime of the validity of χPT and the lattice data.

In this situation it is interesting to consider studies in chiral models —in particular, if they allow to go beyond the range of m_π where χPT is applicable. However, the inevitable prize to pay for the extended range of applicability compared to χPT is model dependence, which introduces hardly controlable systematic uncertainties. Keeping this point critically in mind, such studies may nevertheless provide helpful insights.

In refs. [20–24] the concept was introduced and developed to regularize chiral loops by means of suitable vertex form factors, referred to as "finite-range regulators" (FRR) and intended to simulate physical effects of the pion cloud which has a finite range due to $m_\pi \neq 0$. As argued in [24], the FRR method corresponds in some sense to a (though model-dependent) chiral resummation reliable up to $m_\pi^2 < 1\,\mathrm{GeV}^2$. While being physically intuitive and appealing, the approach was critisized to be unsatisfactory from a field-theoretic point of view, since it gives

[a] e-mail: peter.schweitzer@tp2.ruhr-uni-bochum.de

preference of one ("finite range") regularization scheme to another (*e.g.*, "dimensional") regularization scheme [15].

In this work we address the question how the nucleon mass depends (implicitly) on the pion mass in another effective approach, namely in the chiral quark soliton model (χQSM) [25,26]. This model was derived under certain assumptions from the instanton model of the QCD vacuum [27,28], which provides a dynamical picture of the chiral symmetry breaking mechanism [29]. In this model the nucleon appears as a soliton of the chiral pion mean field in the limit of a large number of colours N_c. The model provides a theoretically consistent description of numerous baryonic quantities ranging from static properties [30,31] over "usual" [32] till "generalized" parton distribution functions [33], which —as far as these quantities are known— agree with phenomenology to within (10–30)% *at the physical point*.

Here —focussing on the nucleon mass M_N— we present the first study in the χQSM at *non-physical pion masses* m_π covering the wide range $0 \leq m_\pi \leq 1500\,\mathrm{MeV}$. We make several remarkable observations. First, stable soliton solutions do exist in this range of pion masses. Second, we demonstrate that the model correctly describes also the heavy quark limit. In the opposite limit $m_\pi \to 0$, which does not commute with large-N_c limit [12,34], the χQSM is known to exhibit a chiral behaviour and to incorporate leading non-analytic terms, which are at variance with the real-world QCD with a finite number of colours $N_c = 3$, but in agreement with its formulation in the limit $N_c \to \infty$ [35–37]. This is consistent as the model is defined in this limit. Third, we show that the χQSM provides a satisfactory description of the *variation* of the lattice data on M_N with m_π in the considered range of pion masses.

Partly, we provide explanations for these observations. Partly, however, they shall remain puzzles to be resolved upon further studies in the model.

This note is organized as follows. In sect. 2 the χQSM is introduced and model results for $M_N(m_\pi)$ are presented, which we compare to lattice QCD in sect. 3. In sect. 4 we discuss the limitations for using the model quantitatively to extrapolate lattice data, and compare in sect. 5 to χPT and the FRR approach. Sect. 6 contains the conclusions. Technical details and a digression on the pion-nucleon sigma-term can be found in the appendices.

2 Pion and nucleon in the effective theory

Let us consider the effective theory which was derived from the instanton model of the QCD vacuum [27,28] and is given by the partition function [38,39]

$$Z_{\rm eff} = \int \mathcal{D}\psi\,\mathcal{D}\bar\psi\,\mathcal{D}U\,\exp\left(i\int \mathrm{d}^4x\;\bar\psi\,(i\partial\!\!\!/ - M\,U^{\gamma_5} - m)\psi\right), \tag{1}$$

where $U = \exp(i\tau^a\pi^a)$ denotes the $SU(2)$ chiral pion field with $U^{\gamma_5} = \exp(i\gamma_5\tau^a\pi^a)$, and M is the dynamical ("constituent") quark mass due to spontaneous breakdown of chiral symmetry, and $m = m_u = m_d$ is the current quark mass. We neglect throughout isospin breaking effects.

The effective theory (1) is valid at low energies below a scale set by the inverse of the average instanton size $\rho_{\rm av}^{-1} \approx 600\,\mathrm{MeV}$. The dynamical mass is momentum dependent, *i.e.* $M = M(p)$, and goes to zero for $p \gg \rho_{\rm av}^{-1}$. In practical calculations it is convenient to replace $M(p)$ by a constant mass M, and to regularize the effective theory within an appropriate regularization scheme with a cutoff $\Lambda_{\rm cut} = \mathcal{O}(\rho_{\rm av}^{-1})$. In the present work we use $M = 350\,\mathrm{MeV}$ from the instanton vacuum model [29].

In the effective theory (1) chiral symmetry is spontaneously broken and a non-zero quark-vacuum condensate $\langle\bar\psi\psi\rangle \equiv \langle\mathrm{vac}|(\bar\psi_u\psi_u + \bar\psi_d\psi_d)|\mathrm{vac}\rangle$ appears which is given in leading order of the large-N_c limit by the quadratically UV-divergent Euclidean loop integral

$$\langle\bar\psi\psi\rangle = -\int \frac{\mathrm{d}^4p_E}{(2\pi)^4}\,\frac{8N_cM'}{p_E^2 + M'^2}\bigg|_{\rm reg} = -8N_cM'I_1(m)\,, \tag{2}$$

where I_1 is its proper-time regularized version, see appendix A, and $M' \equiv M + m$. Note that in QCD strictly speaking $\langle\bar\psi\psi\rangle$ is well defined only in the chiral limit. The pion is not a dynamical degree of freedom in the theory (1). Instead the dynamics of the pion field appears only after integrating out the quark fields which yields the effective action

$$S_{\rm eff}[U] = \frac{f_\pi^2}{4}\int \mathrm{d}^4x\;\mathrm{tr}\;\partial^\mu U\,\partial_\mu U^\dagger + \ldots, \tag{3}$$

where the dots denote the four-derivative Gasser-Leutwyler terms with correct coefficients, the Wess-Zumino term, terms $\propto m$ (and an infinite series of higher-derivative terms) [26]. The pion decay constant $f_\pi = 93\,\mathrm{MeV}$ in eq. (3) is given in the effective theory by the logarithmically UV-divergent loop integral (whose regularized version we denote by I_2, see appendix A)

$$f_\pi^2 = \int \frac{\mathrm{d}^4p_E}{(2\pi)^4}\,\frac{4N_cM'^2}{(p_E^2 + M'^2)^2}\bigg|_{\rm reg} = 8N_cM'^2\;I_2(m)\,. \tag{4}$$

The mass of the pion can be determined from the position of the pole of the pion propagator in the effective theory (1). Its relation to the current quark mass is given by the equation (for the I_i see appendix A)

$$m_\pi^2 = \frac{m}{M}\,\frac{I_1(m)}{I_2(m)}\,, \tag{5}$$

which, for small current quark masses m, corresponds to the Gell-Mann–Oakes–Renner relation

$$m_\pi^2 f_\pi^2 = -m\,\langle\bar\psi\psi\rangle + \mathcal{O}(m^2)\,. \tag{6}$$

The χQSM is an application of the effective theory (1) to the description of baryons [25,26]. The large-N_c limit allows to solve the path integral over pion field configurations in eq. (1) in the saddle point approximation. In the leading order of the large-N_c limit the pion field is static,

and one can determine the spectrum of the one-particle Hamiltonian of the effective theory (1)

$$\hat{H}|n\rangle = E_n|n\rangle\ ,\quad \hat{H} = -i\gamma^0\gamma^k\partial_k + \gamma^0 M U^{\gamma_5} + \gamma^0 m\,. \quad (7)$$

The spectrum consists of an upper and a lower Dirac continuum, distorted by the pion field as compared to continua of the free Dirac-Hamiltonian

$$\hat{H}_0|n_0\rangle = E_{n_0}|n_0\rangle\ ,\quad \hat{H}_0 = -i\gamma^0\gamma^k\partial_k + \gamma^0 M + \gamma^0 m\,, \quad (8)$$

and of a discrete bound-state level of energy $E_{\rm lev}$, if the pion field is strong enough. By occupying the discrete level and the states of the lower continuum each by N_c quarks in an anti-symmetric colour state, one obtains a state with unity baryon number. The soliton energy $E_{\rm sol}$ is a functional of the pion field

$$E_{\rm sol}[U] = N_c\Big[E_{\rm lev} + \sum_{E_n<0}(E_n - E_{n_0})\Big]_{\rm reg}\,. \quad (9)$$

$E_{\rm sol}[U]$ is logarithmically divergent, see appendix A for the explicit expression in the proper-time regularization. By minimizing $E_{\rm sol}[U]$ one obtains the self-consistent solitonic pion field U_c. This procedure is performed for symmetry reasons in the so-called hedgehog ansatz

$$\pi^a(\mathbf{x}) = e_r^a\ P(r)\ ,\quad U(\mathbf{x}) = \cos P(r) + i\tau^a e_r^a \sin P(r)\ , \quad (10)$$

with the radial (soliton profile) function $P(r)$ and $r = |\mathbf{x}|$, $\mathbf{e}_r = \mathbf{x}/r$. The nucleon mass M_N is given by $E_{\rm sol}[U_c]$. The self-consistent profile satisfies $P_c(0) = -\pi$ and decays in the chiral limit as $1/r^2$ at large r. For finite m it exhibits a Yukawa tail $\propto \exp(-m_\pi r)/r$ with the pion mass m_π connected to m by relation (5).

For the following discussion we note that the soliton energy can be rewritten as an expansion in powers of $\partial^\mu U$ as follows:

$$E_{\rm sol}[U] = \sum_{k=1}^{\infty} F_k[(\partial U)^k], \quad (11)$$

where $F_k[(\partial U)^k]$ symbolically denotes a functional in which $\partial^\mu U$ appears k-times (appropriately contracted). Note that in the leading order of the large-N_c limit the soliton field is time independent, *i.e.* ∂U is just ∇U. For some observables the lowest orders in expansions analog to (11) were computed [30–33].

Let us also remark that in the case $m_u = m_d = m_s$ the above given formulae for the soliton energy in the $SU(2)$ version of the model coincide with those from the $SU(3)$ version [31].

In order to describe further properties of the nucleon, it is necessary to integrate over the zero modes of the soliton solution in the path integral, which assigns a definite momentum, and spin and isospin quantum numbers to the baryon. Corrections in the $1/N_c$-expansion can be included by considering time-dependent pion field fluctuations around the solitonic solution. The χQSM allows to evaluate baryon matrix elements of local and non-local QCD quark bilinear operators like $\langle B'|\bar{\Psi}\Gamma\Psi|B\rangle$ (with Γ denoting some Dirac and flavour matrix) with no adjustable parameters. This provides the basis for the wide range of applicability of this model [30–33].

2.1 The mass of the nucleon in the large-N_c limit

If one managed to solve QCD in the limit $N_c \to \infty$ one would in principle obtain for the mass of the nucleon an expression of the form (let the M_i be independent of N_c)

$$M_N = N_c M_1 + N_c^0 M_2 + N_c^{-1} M_3 + \dots\,. \quad (12)$$

The χQSM provides a practical realization of the large-N_c picture of the nucleon [40], and respects the general large-N_c counting rules. In the leading order of the large-N_c limit one approximates in the χQSM the nucleon mass by the expression for the soliton energy in eq. (9), *i.e.* one considers only the first term in the expansion (12) $M_N \approx N_c M_1 = E_{\rm sol}$. We obtain numerically[1]

$$M_N = 1254\,{\rm MeV}, \quad (13)$$

where the cutoff in the regulator function R, see appendix A, is chosen such that for $m_\pi = 140\,{\rm MeV}$ the physical value of the pion decay constant f_π is reproduced. We observe an overestimate of the physical value $M_N = 940\,{\rm MeV}$ by about 30%. This is not surprising, given the fact that we truncate the series in eq. (12) after the first term and thus neglect corrections which are generically of $\mathcal{O}(1/N_c)$, *i.e.* of the order of magnitude of the observed overestimate.

In fact, the soliton approach is known to overestimate systematically the physical values of the baryon masses because of —among others— spurious contributions due to the soliton center-of-mass motion [41]. Taking into account the corresponding corrections, which are $\mathcal{O}(N_c^0)$, reduces the soliton energy by the right amount of about 300 MeV. (Note that there are also other sources of corrections at $\mathcal{O}(N_c^0)$, see ref. [41].) We shall keep in mind this systematic overestimate, when we will discuss lattice data below.

2.2 The chiral limit

In the following we will be interested in particular in the pion mass dependence of the nucleon mass. From χPT we know that

$$M_N(m_\pi) = M_N(0) + A\,m_\pi^2 + B\,m_\pi^3 + \dots\,, \quad (14)$$

where the dots denote terms which vanish faster than m_π^3 with $m_\pi \to 0$. The constants $M_N(0)$ and A (which is related to the pion-nucleon sigma-term) serve to absorb infinite counter-terms in the process of renormalization in χPT —in the sense of renormalizability in χPT. However, the constant B, which accompanies the so-called leading non-analytic (in m, since $m_\pi^3 \propto m^{3/2}$) contribution, is

[1] In this work we quote numerical results to within an accuracy of 1 MeV. However, one should keep in mind that we neglect isospin breaking effects (and electromagnetic corrections). Therefore, we shall round off the physical masses as $m_\pi = 140\,{\rm MeV}$ and $M_N = 940\,{\rm MeV}$, and the same is understood for our numerical results.

finite. For this constant χPT, as well as any theory which correctly incorporates chiral symmetry, yields [12,34]

$$B = k\,\frac{3g_A^2}{32\pi\, f_\pi^2} \tag{15}$$

with $k = 1$ for finite N_c. However, the limits $m_\pi \to 0$ and $N_c \to \infty$ do not commute. If we choose first to take $N_c \to \infty$ while keeping m_π finite, and only then we consider the chiral limit, then $k = 3$. The reason for that is the special role played by the Δ-resonance. In the large-N_c limit the nucleon and the Δ-resonance become mass-degenerated[2]

$$M_\Delta - M_N = \mathcal{O}(N_c^{-1})\,. \tag{16}$$

Taking $N_c \to \infty$ while m_π is kept finite, one has $M_\Delta - M_N \ll m_\pi$ and has to consider the contribution of the Δ-resonance as intermediate state in chiral loops on equal footing with the contribution of the nucleon. The contribution of the Δ-resonance appears (in quantities which do not involve polarization) to be twice the contribution of the nucleon, hence $k = 3$ [37]. This is the situation in the χQSM and, in fact, in this model one recovers [36] the correct (in the large-N_c limit) leading non-analytic term in eq. (15).

2.3 The heavy quark limit

The χQSM is based on chiral symmetry which consideration makes sense only when explicit chiral symmetry breaking effects are small. Nevertheless one can consider the model, in principle, for any value of m. In this context let us first note that taking the limit of a large current quark mass $m \to m_Q$ in eqs. (2), (4), (5) yields, see table 1

$$\lim_{m\to m_Q} m_\pi = 2\,m_Q, \tag{17}$$

which is the correct heavy quark limit for the mass of a meson (see sect. 2.4 on details of parameter fixing).

What happens to the mass of the soliton in this limit? Consider the eigenvalue problem in eq. (7). With increasing $m \to m_Q$ the "potential term" MU^{γ_5} is less and less important and the spectrum of the full Hamiltonian (7) becomes more and more similar to the spectrum of the free Hamiltonian (8). In this limit the eigenvalues of the full and free Hamiltonian nearly cancel in the sum over energies in eq. (9). Only the contribution of the discrete level is not compensated and approaches $E_{\rm lev} \approx m_Q$. Thus, we recover the correct heavy quark limit

$$\lim_{m\to m_Q} M_N = N_c\, m_Q\,. \tag{18}$$

[2] Though in the χQSM one cannot handle $\mathcal{O}(N_c^0)$ corrections to M_N, still one is able to describe consistently the mass difference $(M_\Delta - M_N)$ and to reproduce the large-N_c counting rule in eq. (16) by considering a class of particular (so-called "rotational") $1/N_c$ corrections [28]. In the soliton picture Δ and nucleon are just different rotational states of the same classical soliton. In this note we do not consider rotational corrections and work to leading order in the large-N_c expansion.

Table 1. The dependence on the pion mass for fixed $f_\pi = 93\,\text{MeV}$ in the χQSM. All numbers are in units of MeV. Rows 2,3,4: current quark mass m, cutoff of the effective theory $\Lambda_{\rm cut}$, and quark vacuum condensate $\langle\bar\psi\psi\rangle$ depend on m_π according to eqs. (2), (4), (5). $\Lambda_{\rm cut}$ is of the order of magnitude of the inverse of the average instanton size $\rho_{\rm av}^{-1} \approx 600\,\text{MeV}$. Note that in QCD —in contrast to effective theories with a well-defined regularization prescription— the notion of quark vacuum condensate for $m \neq 0$ is ambiguous. Rows 5,6,7: contributions of the discrete level $N_cE_{\rm lev}$ and the continuum $N_cE_{\rm cont}$ to the total soliton energy $E_{\rm sol} = N_c(E_{\rm lev} + E_{\rm cont})$, see eq. (9), to be identified with the nucleon mass in the model. The numerical numbers confirm within the studied range of m the heavy quark limit discussed in sect. 2.3.

m_π	m	$\Lambda_{\rm cut}$	$-\langle\bar\psi\psi\rangle^{1/3}$	$N_cE_{\rm lev}$	$N_cE_{\rm cont}$	$E_{\rm sol}$
0	0	649	220	681	530	1211
10	0.1	649	220	682	530	1212
50	2	648	220	692	526	1218
140	16	643	218	744	510	1254
300	69	635	211	872	494	1366
600	223	666	204	1202	484	1686
1200	556	799	205	2006	465	2471

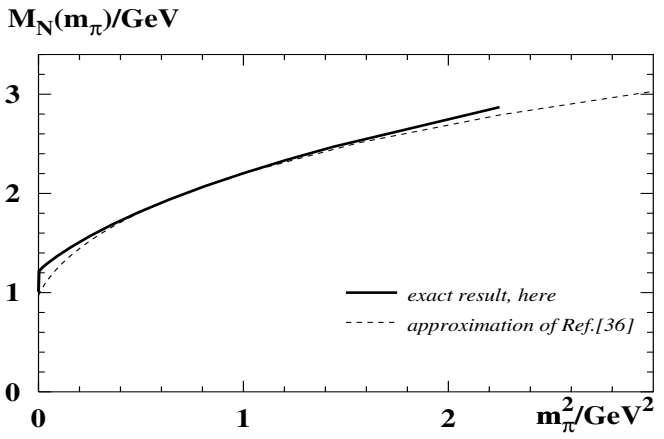

Fig. 1. Nucleon mass $M_N(m_\pi)$ *vs.* m_π^2 in the chiral quark-soliton model. Solid line: exact result obtained here. Dashed line: the approximation based on the instanton vacuum model from ref. [36].

However, the above considerations are formal, since the crucial step consists in demonstrating that a stable soliton solution indeed exists, *i.e.* that a self-consistent profile can be found for which the soliton energy (9) takes a minimum. In practice, we find that stable soliton solutions exist at least up to $m = \mathcal{O}(700\,\text{MeV})$, which is sufficient for a comparison to lattice QCD results. In this range we observe a tendency to approach the limit (18) from below as expected, see table 1. Thus, we find that both the pion and the nucleon mass are correctly described in the effective theory when the current mass of the quarks becomes large.

2.4 Fixing of parameters

When studying the nucleon mass as a function of m_π we must specify what is fixed and what varies in the chiral limit. Here we make the following choice. We keep the dynamical constituent quark mass $M = 350\,\mathrm{MeV}$ and $f_\pi = 93\,\mathrm{MeV}$ fixed. In this way we obtain the results shown in table 1 and plotted as solid line in fig. 1. The meaning of the dashed curve in fig. 1 is explained in appendix B where a digression is given on the pion-nucleon sigma-term related to the slope of $M_N(m_\pi)$.

It should be noted that keeping f_π fixed in the chiral limit is a choice often considered in the literature. However, at this point other choices could be considered as well. *E.g.*, one could fix the pion decay constant to its value $F = 88\,\mathrm{MeV}$ in the chiral limit, or allow f_π to be m_π-dependent, which strictly speaking is the case in χPT and in lattice QCD. In χPT

$$f_\pi(m_\pi) = F\left(1 + \frac{m_\pi^2}{(4\pi F)^2}\,\bar{l}_4 + \mathcal{O}\left(\frac{m_\pi^4}{F^4}\right)\right), \qquad (19)$$

where $\bar{l}_4$ is a low energy constant [13,14]. In lattice calculations f_π increases with larger m_π, exceeding its physical value by about 40% at $m_\pi \sim 1\,\mathrm{GeV}$, *e.g.* [42]. A more consistent way of fixing model parameters could consists in choosing Λ_{cut} (and/or M) such that in the model $f_\pi(m_\pi)$ satisfies (19) with the correct value for $\bar{l}_4$, *and* agrees in each case with lattice results at large m_π.

Remarkably, eq. (19) holds in the model and parameters can be fixed to reproduce $\bar{l}_4$ correctly [35]. However, it is a subtle issue, how to simulate in a chiral model the lattice situation in a realistic way. There a common procedure is to keep fixed all bare lattice parameters but the bare current quark mass (the hopping parameter). In some sense, the dimensionful quantity, which is kept fixed in lattice calculations while m_π "is varied", is the Sommer scale [43] defined by the notion of the heavy quark potential —absent in chiral models.

Notice that the χQSM describes numerous observables to within an accuracy of typically (10–30)% [31], but cannot be expected to be much more precise than that. Overestimating the value of f_π in the chiral limit by 5% or underestimating its lattice values by 30% (or 40%) lies within the accuracy of the model. Note that changing f_π (at non-physical m_π) would alter in particular the values of the cutoff Λ_{cut} and consequently change M_N in table 1. Since f_π and M_N depend on Λ_{cut} logarithmically and thus weakly, these changes may be expected to be small and within the accuracy of the model.

From a practical point of view, our choice to keep f_π fixed to its physical value may be considered as *one* effective prescription, whose consequences one may think absorbed in the unavoidable model dependence of the results.

It would be interesting to consider *other* effective prescriptions which would provide more insights into the model dependence of our study. This is, however, beyond the scope of this work and subject to further investigations [44].

3 Comparison to lattice data

In this section we compare $M_N(m_\pi)$ from χQSM with lattice results on the nucleon mass from refs. [4–11]. Wherever possible we will use only such lattice data, where all bare lattice parameters where kept fixed apart from the current quark mass (or the hopping paramater).

$M_N(m_\pi)$ from the model overestimates the lattice data by about 300 MeV which is expected, if we recall the discussion in sect. 2.1. Remarkably we observe that it is possible to introduce an m_π-*independent* subtraction constant $C = \mathcal{O}(300\,\mathrm{MeV})$ depending on the lattice data, such that $[M_N(m_\pi) - C]$ agrees well with the lattice data.

In fig. 2a we compare the χQSM result for $M_N(m_\pi)$ to full lattice data by the UKQCD and QCDSF Collaborations [6,7] obtained from simulations on $(16\text{–}24)^3 \times 48$ lattices using the standard Wilson plaquette action for gauge fields and the non-perturbatively $\mathcal{O}(a)$ improved action for fermions. The fat points in fig. 2a were extracted from simulations at $5.20 \le \beta \le 5.29$ on lattices of the physical size $L \ge 1.96\,\mathrm{fm}$ with $m_\pi L > 6$ and lattice spacings $a = 0.09\,\mathrm{fm}$ to $0.12\,\mathrm{fm}$ fixed by the Sommer method with $r_0 = 0.5\,\mathrm{fm}$ [43]. Other lattice spacings quoted below were also determined by means of this popular method which, however, is not free of criticism [45]. A best fit yields $C = 329\,\mathrm{MeV}$ with a χ^2 per degree of freedom of $\chi^2_{\mathrm{dof}} = 0.7$ and is shown in fig. 2a. The uncertainty of the constant C due to the statistical error of the lattice data is of the order of magnitude of few MeV, see table 2, and thus negligible, see the remarks in footnote 1.

For comparison in fig. 2a also data by the UKQCD and QCDSF Collaborations [6,7] are shown from smaller lattices $L = 1.5\,\mathrm{fm}$ to $1.7\,\mathrm{fm}$. Finite-size effects are clearly visible, and were subject to a detailed study in ref. [7]. Since the present χQSM calculation by no means is able to simulate finite-volume effects, we restrict our study to data from lattices with $L \gtrsim 2\,\mathrm{fm}$. The study of ref. [7] indicates that for lattices of this size finite-volume effects can be assumed to be small. Also, in this work we consider data obtained from lattices with spacings $a \le 0.13\,\mathrm{fm}$ and assume discretization effects to be negligible. Such effects are difficult to control systematically [46].

In fig. 2b the χQSM result for $M_N(m_\pi)$ is compared to lattice data by the JLQCD Collaboration from ref. [5], where dynamical simulations with two flavours were performed on a $20^3 \times 48$ lattice using the plaquette gauge action and the non-perturbatively $\mathcal{O}(a)$ improved Wilson quark action at $\beta = 5.20$ with lattice spacings $0.10\,\mathrm{fm} \le a \le 0.13\,\mathrm{fm}$. The physical size of the lattice was $1.96\,\mathrm{fm} \le L \le 2.53\,\mathrm{fm}$ and the range $500\,\mathrm{MeV} \le m_\pi \le 1\,\mathrm{GeV}$ was covered corresponding to $m_\pi L > 5$. The best fit yields $C = 341\,\mathrm{MeV}$ with a $\chi^2_{\mathrm{dof}} = 0.3$ and is shown in fig. 2b.

In figs. 2c and d we compare $M_N(m_\pi)$ from the model to lattice results by the CP-PACS Collaboration [4], which were obtained on $24^3 \times 48$ lattices from a renormalization-group improved gauge action and a mean-field improved clover quark action at $\beta = 2.1$ (and $\beta = 2.2$) with dynamical u- and d-quarks and quenched s-quarks. For hadrons with no valence s-quarks this practically means a full two-flavour simulation. The physical lattice spacings and sizes

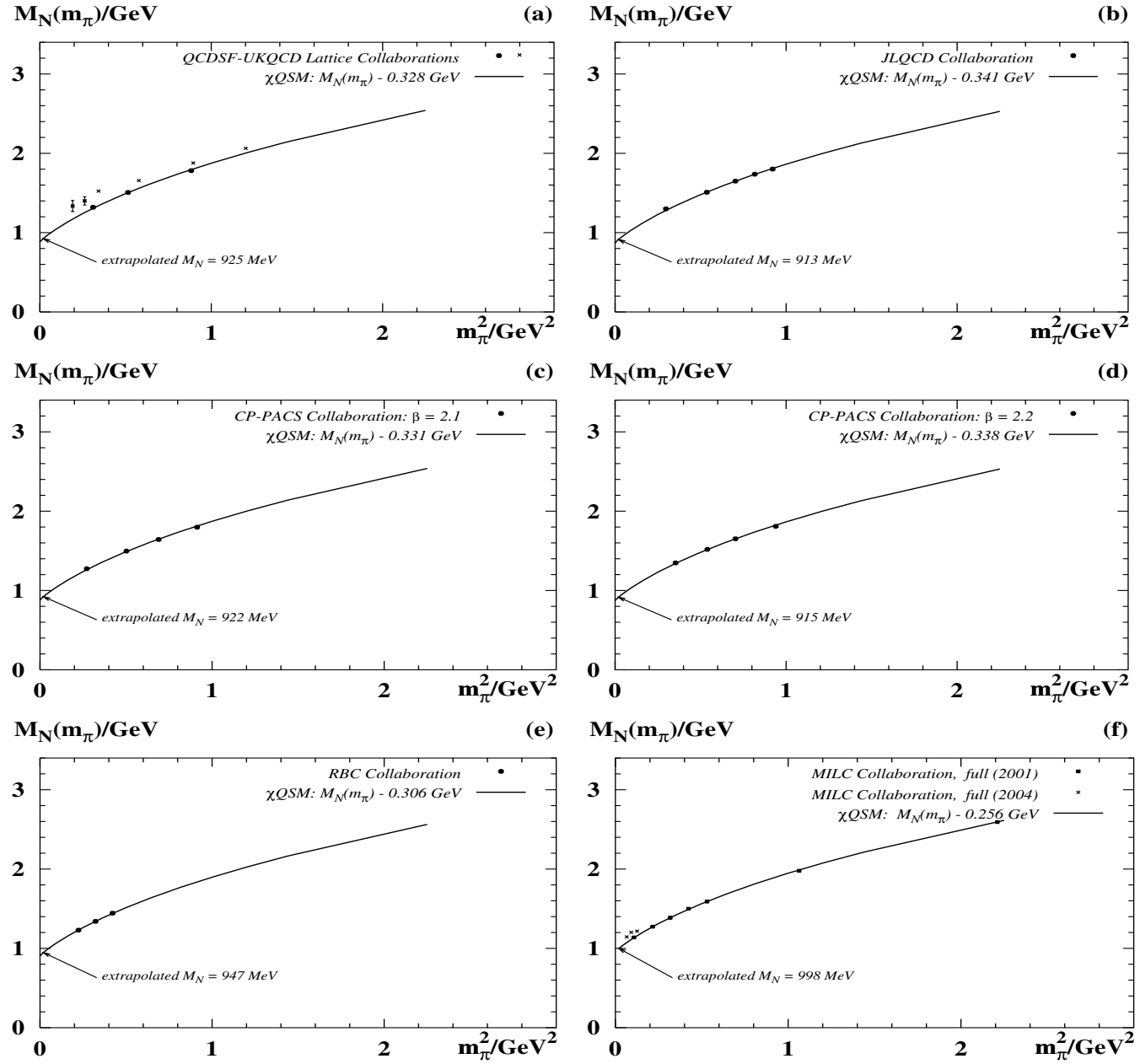

Fig. 2. $M_N(m_\pi)$ *vs.* m_π^2 from the chiral quark-soliton model *vs.* lattice data on $M_N(m_\pi)$ from full simulations by (a) the UKQCD-QCDSF Collaborations [6,7], (b) the JLQCD Collaboration [5], (c,d) the CP-PACS Collaboration [4], (e) the RBC Collaboration [8], (f) the MILC Collaboration [9,10]. All data were obtained from large lattices $L \gtrsim 2\,\mathrm{fm}$, with the exception of the data marked by crosses in (a), see text. Unless error bars are shown, here and in the following figures the statistical error of the lattice data is comparable to or smaller than the size of the points in the plot.

were $a = 0.09\,\mathrm{fm}$ to $0.13\,\mathrm{fm}$ and $L = 2.22\,\mathrm{fm}$ to $3.12\,\mathrm{fm}$ with pion masses in the range $500\,\mathrm{MeV} \leq m_\pi \leq 1\,\mathrm{GeV}$, such that $m_\pi L \gtrsim 7$. We observe that $M_N(m_\pi)$ from the χQSM with a subtraction constant $C = 331\,\mathrm{MeV}$ with $\chi^2_{\mathrm{dof}} = 2.2$ (and $C = 338\,\mathrm{MeV}$ with $\chi^2_{\mathrm{dof}} = 0.4$) describes well the lattice data of ref. [4], see figs. 2c and d.

Next, we confront the model results for $M_N(m_\pi)$ to lattice data from dynamical two-flavour simulations with domain wall fermions by the RBC Collaboration [8], which have the virtue of preserving chiral invariance. In ref. [8] a renormalization group improved ("doubly blocked Wilson") gauge action with $\beta = 0.80$ was used on a $16^3 \times 32$ lattice with the physical spacing of 0.12 fm and a lattice size about 2 fm. The range of pion masses was $m_\pi = 470\,\mathrm{MeV}$ to $650\,\mathrm{MeV}$. The best fit yields for the constant $C = 306\,\mathrm{MeV}$ with $\chi^2_{\mathrm{dof}} = 0.02$, and provides a very good description of the data, see fig. 2e.

In fig. 2f we compare $M_N(m_\pi)$ from the χQSM with 2001 lattice data by the MILC Collaboration [9] obtained from simulations with three dynamical quarks using a one-

Table 2. Comparison of the $M_N(m_\pi)$ obtained from the χQSM to the lattice data [4–11]. For convenience we quote the lattice sizes and spacings and the range of m_π covered in the lattice simulations in physical units which were fixed by the Sommer method [43]. The soliton approach generally overestimates [41] the nucleon mass at the physical point by about 300 MeV, see eq. (13). We find a similar overestimate at the respective lattice values of m_π. Correcting for this overestimate by introducing a m_π-independent subtraction constant C to be fitted to the respective lattice data set, we observe a good agreement $[M_N(m_\pi)-C]$ with the lattice data, see figs. 2 and 3. The 5th row shows the fit results for the constant C and its 1-σ uncertainty due to the statistical error of the lattice data, and the 6th row shows the χ^2 per degree of freedom ($\chi^2_{\rm dof}$) of the respective fit. Also the "extrapolated" (within the χQSM) value of the nucleon mass at the physical point (M_N) is included. It has the same uncertainty as the fit-constant C, which is due to the statistical error of lattice data and practically negligible, see the remark in footnote 1. It has also an unestimated systematic error due to model-dependence, see sect. 4.

Collaboration	Lattice size/fm	Spacing/fm	m_π-range/MeV	C/MeV	$\chi^2_{\rm dof}$	M_N/MeV
UKQCDSF [6,7]	2.0–2.2	0.09–0.12	550–940	329 ± 7	0.7	925
JLQCD [5]	2.0–2.5	0.10–0.13	540–960	341 ± 7	0.3	913
CP-PACS [4] ($\beta = 2.1$)	2.7–3.1	0.11–0.13	520–960	331 ± 4	2.2	922
CP-PACS [4] ($\beta = 2.2$)	2.2–2.4	0.09–0.10	590–970	338 ± 6	0.4	915
RBC [8]	1.9–2.0	0.12	470–650	306 ± 11	0.02	947
MILC [9] (all data)	2.6	0.13	350–1500	256 ± 2	1.2	998
MILC [9] (only $m_{u,d} = m_s$)	2.6	0.13	720–1500	260 ± 3	1.9	993
CSSM [11] (quenched)	2.0	0.125	540–920	345 ± 5	1.3	909

loop Symanzik improved gauge action and an improved Kogut-Susskind quark action. The physical lattice size was tuned to $L = 2.6\,$fm with a lattice spacing of 0.13 fm and the range of pion masses $340\,\text{MeV} \leq m_\pi \leq 2.2\,\text{GeV}$ was covered. The best fit yields $C = 256\,$MeV for the subtraction constant (with $\chi^2_{\rm dof} = 1.2$).

One could worry whether the $SU(2)$ model results can be compared to three-flavour lattice simulations, though in [9] for the nucleon mass no significant differences were noticed between two- and three-flavour runs. However, as noted in sect. 2, the nucleon mass is the same in the $SU(2)$ and $SU(3)$ versions of the χQSM if $m_u = m_d = m_s$, which is the case for the lattice data [9] for $m_\pi > 700\,$MeV. Restricting the fitting procedure to this range of m_π (the last three points in fig. 2f) we obtain $C = 260\,$MeV (with $\chi^2_{\rm dof} = 1.9$). This fit is shown in fig. 2f. Note that it is practically indistinguishable, cf. footnote 1, from the fit where the whole m_π-range (*i.e.* also data with $m_u = m_d < m_s$) was used, and it equally well describes the region of lower m_π. In any case we observe a good agreement with the lattice data [9] up to $m_\pi = 1.5\,$GeV.

We include in fig. 2f also the recent small-m_π (2004) MILC data [10] from the "coarse" lattices with $L = 20$ (or $L = 24$ for the lowest m_π-value) which have a lattice spacing $a \approx 0.12\,$fm comparable to [9]. These data are not compatible with the χQSM result. In this context it is important to note that the simulation for the highest m_π-value of the 2004 MILC data [10] is an extended run of the simulation for the lowest m_π of the 2001 data [9]. One would therefore expect that they coincide in the plot in fig. 2f, which is not the case. In fact, the MILC data [9, 10] for this particular simulation are well consistent with each other in *lattice units*: am_π and aM_N from these runs agree within statistical error bars.

The discrepancy of the results from [9,10] in fig. 2f is due to the different values for r_1 —a parameter defined similarly to the Sommer scale r_0 and used to fix the physical units in [9,10]. Different methods were used to determine the physical unit of r_1 —resulting in the value $r_1 = 0.35\,$fm in [9], and $r_1 = 0.324(4)\,$fm in [10]. Had we used the r_1-value from [9] to give physical units to the dimensionless lattice numbers for am_π and aM_N from [10], then the two data sets would perfectly agree in fig. 2f, and the 2004 data would be compatible with the χQSM results. The precise determination of the physical units of lattice data is a difficult issue [43,45], see also [9,10].

It is instructive to compare the model results also to lattice data obtained from simulations performed in the *quenched* approximation, *e.g.*, by the CSSM Lattice Collaboration [11], where a mean-field improved gauge action and a fat-link clover fermion ("FLIC") action was used on a $16^3 \times 32$ lattice with a lattice spacing of $a = 0.125\,$fm. The calculation covers the range $540\,\text{MeV} \leq m_\pi \leq 920\,\text{MeV}$. A best fit to the quenched data gives $C = 345\,$MeV (with a $\chi^2_{\rm dof} = 1.3$) which yields a good agreement with the lattice data, see fig. 3a.

For the quenched data by the MILC Collaboration [9], however, we observe that a fit would work much worse. In this case we refrain from fitting and show instead in fig. 3b the fit to the full MILC data from fig. 2f, which nicely illustrates how results from full and quenched calculations differ. Interestingly, at large m_π^2 the full and quenched data of ref. [9] agree well with eachother. In fact, it is not suprising that differences between full and quenched simulations become less pronounced with increasing m_π^2, *i.e.* with increasing fermion masses.

Thus, we observe that the χQSM result for $M_N(m_\pi)$ supplemented by an m_π-independent subtraction constant C (whose precise value follows from a best fit to the respective lattice data) is able to describe the lattice data [4–11] over a wide range of pion masses $350\,\text{MeV} \leq m_\pi \leq 1500\,\text{MeV}$. The results are shown in figs. 2 and 3 and are summarized in table 2.

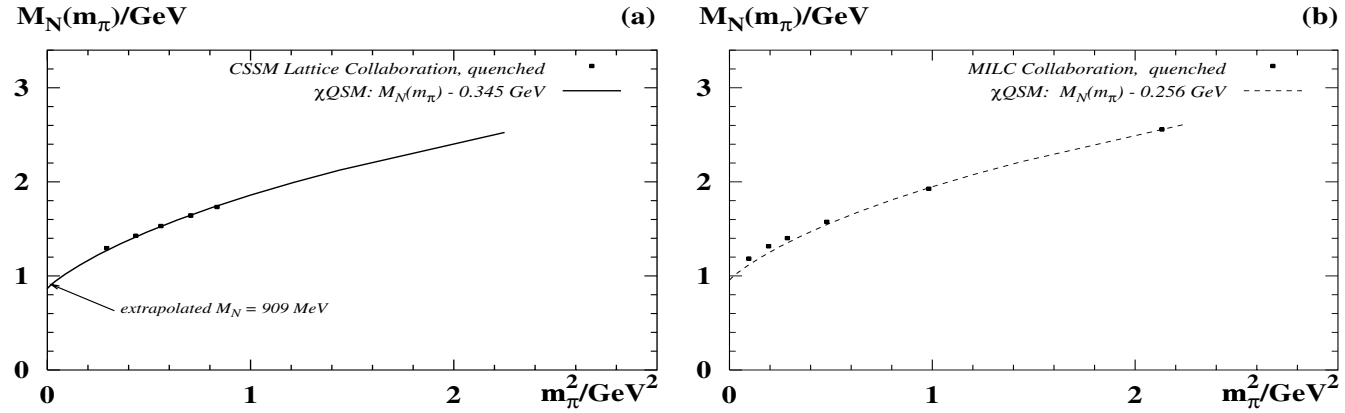

Fig. 3. $M_N(m_\pi)$ *vs.* m_π^2 from the chiral quark-soliton model *vs.* lattice data on $M_N(m_\pi)$ obtained in the quenched approximation by (a) the CSSM Lattice Collaboration [11] and (b) the MILC Collaboration [9].

4 χQSM as tool for extrapolation?

From the $[M_N(m_\pi) - C]$ at $m_\pi = 140\,\mathrm{MeV}$ with the constant C fitted to the respective data, we can read off in principle the physical value of the nucleon mass —"extrapolated" from the respective lattice data by means of the χQSM as a guideline. These extrapolated values are indicated by arrows in figs. 2a-f and 3a, and are summarized in table 2.

It is worthwhile stressing that the extrapolated values in table 2 agree within an accuracy of $\pm 5\%$ with the physical nucleon mass. (Though at the same time, lattice data for f_π are underestimated by up to 40% at large $m_\pi \sim 1\,\mathrm{GeV}$, see sect. 2.4.) The uncertainty of the extrapolated values for the nucleon mass is the same as for the fit constant C as quoted in table 2, *i.e.* it is of the order of few MeV and thus negligible, see footnote 1.

However, what does not need to be negligible, is the systematic error of such an extrapolation. First of all, this extrapolation is done within the χQSM, and the results are model dependent. *E.g.*, handling the model parameters in the chiral limit differently would change our results —though one may expect a qualitatively similar picture, see the discussion in sect. 2.4. Apart from this source of model dependence, which will be subject to future numerical studies [44], there are principal difficulties to estimate reliably the systematic error within the model, as we shall see in the following.

Let us first address the question of the range of reliability of the χQSM description of $M_N(m_\pi)$. For that it is instructive to compare to χPT and the effective FRR approach. χPT to $\mathcal{O}(p^4)$ was argued to provide a reliable expansion for $M_N(m_\pi)$ up to $m_\pi^2 < 0.4\,\mathrm{GeV}$ [15–18] (p is to be identified with the generic small expansion parameter in χPT, *e.g.*, in our context pion mass). A more conservative bound $m_\pi^2 < 0.1\,\mathrm{GeV}^2$ was given in [19]. The effective FRR approach was argued to correspond to a *partial* resummation of the chiral expansion, and to be valid up to $m_\pi^2 < 1\,\mathrm{GeV}^2$ [24] (which comes, of course, at the prize of introducing model dependence, see the discussion in sect. 1).

What might be the range of reliability of the χQSM? Recall that the χQSM expression for the nucleon mass (as well as for any other quantity) may be considered as a resummed infinite series in derivatives of the chiral field $U = \exp(i\tau^a\pi^a)$, cf. eq. (11), whereby it is understood that each chiral order is evaluated in the large-N_c limit. (Keep in mind that these limits do not commute, see sect. 2.2.) Thus, one may argue that the χQSM corresponds to a chiral expansion, which is *completely* resummed —to leading order of the large-N_c expansion. If one were happy with this approximation, then χQSM results could be considered reliable for all m_π including the heavy quark limit, see the discussion in sect. 2.3. It must be stressed, that —as in the case of the FRR approach— this chiral resummation is performed *within* a particular model of the nucleon. Thus, our results and conclusions are inevitably model dependent.

The wide range of reliability of the χQSM we observe in practice is illustrated in fig. 4, where we show the χQSM-fit to the MILC lattice data [9] and the χPT-fit from [17]. (For further details see sect. 5.)

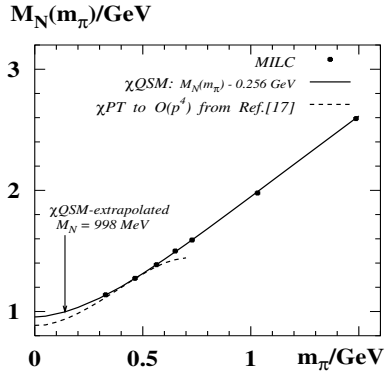

Fig. 4. Lattice data by MILC [9] on $M_N(m_\pi)$ *vs.* m_π and the fits to these data in χPT from ref. [17] (where the physical value of M_N was used as input) and in the χQSM, cf. fig. 2f. The figure illustrates the wide range of applicability of the χQSM.

The perhaps most serious restriction might be that the χQSM assumes the number of colours N_c to be large. What might be the effects due to $1/N_c$ corrections?

Let us consider the mass difference between the Δ-resonance and the nucleon as a measure for such corrections. Note that this mass difference vanishes not only in the large-N_c limit, see eq. (16), but also in the heavy quark limit [34]. This is supported by lattice results [4, 9,11], where always $\Delta \equiv M_\Delta - M_N < m_\pi$ holds. (This means that on present day lattices the Δ-resonance is safe from strong decays and thus a stable particle.) In the region $m_\pi^2 > 0.32\,\mathrm{GeV}^2$ one finds $\Delta < \frac{1}{5} m_\pi$ [4,9,11]. Thus, practically for most of the present-day lattice data the condition

$$\Delta \equiv M_\Delta - M_N \ll m_\pi \quad \text{for } m_\pi^2 > 0.32\,\mathrm{GeV}^2 \tag{20}$$

is satisfied, such that the Δ-nucleon mass difference can be neglected to a good approximation. This may be a reason for the good description of lattice data in the χQSM up to $m_\pi^2 \leq 2.3\,\mathrm{GeV}^2$ in sect. 3.

However, in the physical region $\Delta = 290\,\mathrm{MeV}$ is larger than $m_\pi = 140\,\mathrm{MeV}$, and the leading-order large-N_c treatment of the nucleon mass inevitably introduces a serious systematic error. In fact, one could express the nucleon mass as a function of m_π and $y = \Delta/m_\pi$ as

$$M_N(m_\pi, \Delta) = F(m_\pi, y), \qquad y = \frac{\Delta}{m_\pi}\,. \tag{21}$$

Then, using the χQSM as a guideline for the extrapolation of lattice data corresponds to approximating

$$M_N = F(m_\pi, 2.1) \approx F(m_\pi, 0) \quad \text{at } m_\pi = 140\,\mathrm{MeV}. \tag{22}$$

It is difficult to quantify the systematic error associated with this approximation. A very rough estimate of this error within the model is given in appendix C.

Finally, let us discuss the role of the subtraction constant C. As mentioned in sect. 2 the appearence of such a constant is theoretically well motivated and understood in the soliton approach [41]. The comparison to lattice data indicates that this constant is about $C = \mathcal{O}(300\,\mathrm{MeV})$ and m_π-independent in the covered m_π-range within the statistical accuracy of the lattice data, see table 2. Although this happens to be the magnitude for this constant needed for the model result to coincide with the physical value of the nucleon mass, see eq. (13), it would be premature to assume the constant C to be m_π-independent for all m_π. However, this is what we implicitly did when quoting the extrapolated values for M_N in table 2. The question, whether or not the constant C is m_π-dependent, cannot be answered rigorously within the model.

As an intermediate summary, we conclude that besides the general drawback of being model dependent, the use of the χQSM as a guideline for an extrapolation of lattice data is limited by two major sources of systematic error, namely $1/N_c$ corrections and a possible m_π-dependence of the constant C. Both are not under control within the model and prevent a reliable estimate of the systematic error of the extrapolation. At this point it is instructive to compare to χPT and the FRR model, which may give us a rough idea about the size of the systematic effects.

5 Comparison to χPT and FRR

In order to test the results from the χQSM below the m_π-range available from lattice QCD we have to compare to χPT which allows to connect model independently lattice data through the physical point to the chiral limit. In the following we shall focus on the analyses [7,16,17] in χPT up to $\mathcal{O}(p^4)$ (and refer to them simply as χPT). To this order the chiral expansion of the nucleon mass is characterized by 4 low-energy constants —or more precisely, by 4 linearly independent combinations of them. These constants are in principle known from studies of nucleon-nucleon or pion-nucleon low-energy scattering data. However, they can alternatively be determined from a fit to lattice data.

Figure 5a shows the $M_N(m_\pi)$ as obtained in χPT from fits to the lattice data [4–7] satisfying $a < 0.15\,\mathrm{fm}$, $m_\pi L > 5$ and, respectively, the constraint $m_\pi < 800\,\mathrm{MeV}$ in ref. [7], and $m_\pi < 600\,\mathrm{MeV}$ in ref. [16]. Also shown in fig. 5a is the fit of ref. [17] to the MILC data [9], where a simultaneous fit to lattice data on $M_\Delta(m_\pi)$ was performed. In [16,17] the physical values of the nucleon and/or Δ-mass were included as constraints to the fit. Note that low-energy constants resulting from the different fits [7, 16,17] are compatible with the respective phenomenological values. From this point of view the different lattice data in fig. 5a are consistent with each other. For comparison in fig. 5a our χQSM-fits to the same data sets are shown.

Notice that the two highest-m_π data points (marked by empty circles in fig. 5a) by the UKQCD Collaboration [6,7] were obtained from somehow smaller lattices of the size $L = 1.56\,\mathrm{fm}$ and $1.68\,\mathrm{fm}$ and clearly do not follow the tendency of the $M_N(m_\pi)$ from the χQSM. These points are therefore omitted from the fit shown in fig. 5a. Including these points significantly worsens the χ^2_{dof} of the fit, see table 3 where the results are summarized. Since the χQSM description of the lattice data effectively works also at significantly larger m_π, see sects. 3 and 4 and cf. fig. 4, we conclude that, quoting ref. [16], "*the surprizingly good (and not yet understood) agreement with lattice data (above $m_\pi > 600\,\mathrm{MeV}$) even up to $m_\pi \approx 750\,\mathrm{MeV}$*" is an accidental consequence of comparing χPT to $\mathcal{O}(p^4)$ at the edge (if not above) of its range of applicability to lattice data where finite-size effects start to play a role.

In fact, up to $m_\pi \lesssim (500\text{–}550)\,\mathrm{MeV}$ the χPT to $\mathcal{O}(p^4)$ [7,16,17] and the χQSM describe $M_N(m_\pi)$ in good qualitative agreement, see fig. 5a. Beyond this point, however, the nucleon mass as a function of m_π^2 from χPT in refs. [7,16] changes the curvature, indicating that the range of reliability of χPT to $\mathcal{O}(p^4)$ could be $m_\pi \lesssim 500\,\mathrm{MeV}$ (which, in fact, is not far from the generally assumed bound $m_\pi < 600\,\mathrm{MeV}$). This contrasts the χQSM result exhibiting, in agreement with lattice data, negative curvature up to the highest considered m_π^2.

With the above considerations in mind, we conclude that the χQSM describes lattice data [4–7] constrained by $a < 0.15\,\mathrm{fm}$, $m_\pi L > 5$ and $L \geq 2\,\mathrm{fm}$ very well, see fig. 5a and cf. fig. 4. In the range below $m_\pi \lesssim 500\,\mathrm{MeV}$ we observe a good qualitative and quantitative agreement of

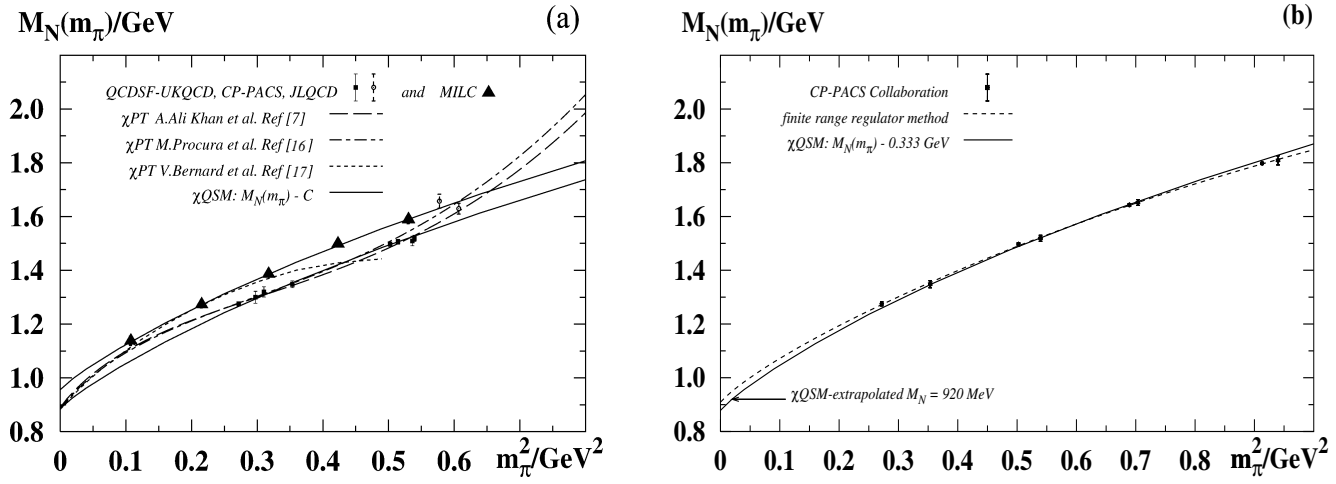

Fig. 5. (a) Selected lattice data on $M_N(m_\pi)$ by QCDSF-UKQCD, CP-PACS, JLQCD [4–7] and the corresponding fits in χPT to $\mathcal{O}(p^4)$ from refs. [7,16], in comparison with lattice data by MILC [9] and the fit in χPT to $\mathcal{O}(p^4)$ from ref. [17]. (b) Lattice data by CP-PACS [4] and the fit in the finite-range regulator approach (with a dipole regulator) [24]. In both figures the respective χQSM-fits are shown.

Table 3. The value of the physical nucleon mass M_N as extrapolated by means of χPT to $\mathcal{O}(p^4)$ lattice data [4–7] subject to the constraints $a < 0.15\,\text{fm}$, $m_\pi L > 5$ and, respectively, $m_\pi < 800\,\text{MeV}$ in ref. [7], and $m_\pi < 600\,\text{MeV}$ in ref. [16]. For comparison the χQSM-fits to the same data set, and to the same data set subject to the additional condition $L \geq 2\,\text{fm}$ are shown. The error of M_N due to the statistical uncertainty of the lattice data and the χ^2_{dof} of the fit are shown. The systematic error of M_N due to the extrapolation method, as well as lattice discretization or finite-size effects, is merely indicated. (See the remark in footnote 1 concerning the small error of the χQSM-fit due to the statistical uncertainty of lattice data.)

Method	M_N in MeV	χ^2_{dof}
χPT to $\mathcal{O}(p^4)$, "Fit I" in ref. [7]	$948 \pm 60 \pm$ syst	1.7
χPT to $\mathcal{O}(p^4)$, "Fit II" in ref. [16]	938 (fixed)	–
χQSM (only $L \gtrsim 2\,\text{fm}$)	$927 \pm 4 \pm$ syst	0.5
χQSM (all data points)	$931 \pm 4 \pm$ syst	2.3

the χQSM with χPT to $\mathcal{O}(p^4)$ [7,16,17]. In this range the curves for $M_N(m_\pi)$ from the two approaches agree with each other to within an accuracy of 50 MeV and better, see figs. 4 and 5a. This number may give us a flavour of the magnitude of the systematic error of the χQSM extrapolation of lattice data, though χPT to $\mathcal{O}(p^4)$ may also have such an intrinsic uncertainty, as indicated in table 3, due to unestimated contributions from $\mathcal{O}(p^5)$.

Next, we consider the effective approach based on the finite-range regulator (FRR) method of ref. [24]. There 5 free parameters appear, which can well be constrained by lattice data thanks to the larger range of applicability of the approach, namely up to $m_\pi^2 = 1\,\text{GeV}^2$. In ref. [24] different shapes of regulators were exploited and shown to yield practically the same results. Figure 5b shows the 5-parameter fit (using the dipole-type regulator) to the CP-PACS lattice data sets with $\beta = 2.1$ and 2.2 from ref. [4]. In the χQSM approach with one free parameter only, we were able to fit both data sets separately, see figs. 2c and d. For the sake of comparison we include the combined χQSM-fit in fig. 5b and summarize the results in table 4.

Table 4. The value of the physical nucleon mass M_N as extrapolated from CP-PACS lattice data [4] obtained from lattices of the sizes $L = (2.2\text{–}3.1)\,\text{fm}$ with lattice spacings $a = (0.09\text{–}0.13)\,\text{fm}$ covering the range $520\,\text{Mev} \leq m_\pi \leq 970\,\text{MeV}$. As guidelines for the extrapolation the finite-range regulator approach [24] and the χQSM were used. See also the remarks in the caption to table 3.

Method	M_N in MeV	χ^2_{dof}
Finite-range ("dipole") regulator [24]	$959 \pm 116 \pm$ syst	0.4
χQSM	$920 \pm 3 \pm$ syst	1.2

As demonstrated in fig. 5b and table 4 the results for $M_N(m_\pi)$ from the FRR approach and the χQSM describe the CP-PACS data [4] equally well. Having a closer look on the region $m_\pi^2 < 0.3\,\text{GeV}^2$ we see that $M_N(m_\pi)$ from the χQSM starts to deviate more and more strongly from the fit of the FRR approach with decreasing m_π^2, though the curves remain very similar. The reason for the discrepancy (which apparently was of no relevance for $m_\pi^2 > 0.3\,\text{GeV}^2$, see fig. 5b) should be attributed to the fact that $M_\Delta - M_N$ is kept finite in the FRR approach, but neglected in the χQSM.

Thus one is led to the conclusion that the FRR method and the χQSM are completely consistent modulo $1/N_c$ corrections.

At the physical point the difference between the values of M_N extrapolated by means of the FRR method

and the χQSM is about 40 MeV, which again may give us a rough idea on the theoretical uncertainty due to neglecting the Δ-nucleon mass difference. Note that for this rough estimate we use the central value of the extrapolated M_N from the FRR approach, see table 4, which has a substantially larger statistical uncertainty arising from fitting 5 parameters to the lattice data. In this respect the χQSM-fit is far more precise.

To summarize, the comparison of the χQSM-based fits and those obtained using the first-principle approach in χPT [7,16] and the FRR approach [24] leads us to the following conclusion. The systematic uncertainty of M_N due to neglecting the finite Δ-nucleon mass-splitting in the χQSM is effectively of the order of magnitude of 50 MeV with the tendency to underestimate the nucleon mass. Noteworthy, a similar result —concerning both sign and order of magnitude— follows from a crude estimate within the model itself, see appendix C.

Recall that we did not consider isospin breaking effects or electromagnetic corrections $\sim \mathcal{O}(10\,\mathrm{MeV})$, see footnote 1. Including this we have to assign a systematic error to the χQSM-fits of about $(\delta M_N)_{\mathrm{syst}} \approx 60\,\mathrm{MeV}$. Taking into account a systematic error of this magnitude we observe that the extrapolated values in tables 2, 3 and 4 are all consistent with the physical mass of the nucleon.

We stress that we do not see any possibility to quantify the uncertainty of the χQSM extrapolation of lattice data more quantitatively than that.

6 Conclusions

The implicit dependence of the nucleon mass M_N on the pion mass m_π was studied in the large-N_c limit in the framework of the chiral quark soliton model. The $M_N(m_\pi)$ in the model exhibits a chiral behaviour and includes leading non-analytic terms which are consistent with the large-N_c formulation of QCD [36]. As was shown here, the model describes correctly also the heavy quark limit. The most remarkable observation we make here is that the model results for $M_N(m_\pi)$ well describe lattice data from full simulations [3–9] over the wide range of pion masses $0.1\,\mathrm{GeV}^2 < m_\pi^2 < 2.5\,\mathrm{GeV}^2$, provided one takes into account the generic overestimate of the nucleon mass in the soliton approach [41]. This is done by introducing an m_π-independent subtraction constant, *i.e.* one single parameter to be fitted to the respective lattice data set.

The good description of the lattice data on $M_N(m_\pi)$ can *partly* be understood as follows. In the χQSM, in the leading order of the large-N_c limit, the Δ-nucleon mass-splitting $\Delta = M_\Delta - M_N \sim \mathcal{O}(N_c^{-1})$ is neglected. That is a reasonable approximation when comparing to the present-day lattice simulations where $\Delta^2 \ll m_\pi^2$ holds. However, the remarkable precision, to which the model describes the lattice data, remains a puzzle —to be clarified by further model studies.

We observe that the values for the nucleon mass "extrapolated" from the lattice data [3–9] on the basis of results from the χQSM are in good agreement with extrapolations based on the first-principle approach in χPT [7,16] or the effective FRR approach of ref. [24], and agree with the physical nucleon mass to within 5%. (But one has to keep in mind that at the same time —for the adopted handling of model parameters in the chiral limit— the lattice values of the pion decay constant at large $m_\pi \sim 1\,\mathrm{GeV}$ are underestimated by up to 40%.)

It is difficult to exactly quantify the theoretical uncertainty of this extrapolation due to the model dependence. The main limitation for using the χQSM as a guideline for the chiral extrapolation of lattice data is due to the large-N_c limit. There is no strict control within the model of the theoretical uncertainty introduced by neglecting the finite Δ-nucleon mass-splitting at the physical point, and we cannot quantify this and other uncertainties due to model dependence quantitatively. This limits the use of the model as a *quantitative* effective tool for the extrapolation of lattice data.

Still, the model may provide interesting *qualitative* insights —in particular in those cases when the matching between lattice results and χPT is difficult. A prominent example for that are (moments of) structure functions. In order to use the χQSM as a qualitative, but within its model accuracy reliable device, which is helpful for a comparison of lattice results to experimental data, further model studies are necessary —concerning the issue of handling model parameters in the chiral limit as well as addressing other observables [44].

From the model point of view the observations made in this work also contribute to a better understanding of the physics which underlies the chiral quark-soliton model, and may —that is our hope— stimulate further studies in this direction in this, and perhaps also other models.

We thank Dmitri Diakonov, Thomas Hemmert, Victor Petrov, Pavel Pobylitsa, Maxim Polyakov, Gerrit Schierholz, Wolfram Schroers and Tony Thomas for fruitful discussions and valuable comments. This research is part of the EU integrated infrastructure initiative hadron physics project under contract number RII3-CT-2004-506078, and partially supported by the Graduierten-Kolleg Bochum-Dortmund and Verbundforschung of BMBF. A.S. acknowledges support from GRICES and DAAD.

Appendix A. Proper-time regularization

The proper-time regularized versions of the integrals I_1 and I_2 appearing in eqs. (2), (4) are given by

$$I_1(m) = \int_{\Lambda_{\mathrm{cut}}^{-2}}^{\infty} \frac{\mathrm{d}u}{u^2}\, \frac{\exp(-uM'^2)}{(4\pi)^2}\,, \tag{A.1}$$

$$I_2(m) = \int_{\Lambda_{\mathrm{cut}}^{-2}}^{\infty} \frac{\mathrm{d}u}{2u}\, \frac{\exp(-uM'^2)}{(4\pi)^2} \int_0^1 \mathrm{d}\beta \exp(u\beta(1-\beta)m_\pi^2),$$

where the m-dependence is hidden in $M' \equiv M + m$. For a given m_π and $f_\pi = 93\,\mathrm{MeV}$ fixed and due to eqs. (4), (5) both the current quark mass and the cutoff are (implicit) functions of m_π, *i.e.* $m = m(m_\pi)$ and $\Lambda_{\mathrm{cut}} = \Lambda_{\mathrm{cut}}(m_\pi)$; some selected values are shown in table 1.

The expression for the soliton energy (9) in the proper-time regularization is given by

$$E_{\rm sol} = N_c\Big[E_{\rm lev} + \sum_n \big(R(E_n) - R(E_{n_0})\big)\Big]\,;$$
$$R(\omega) = \frac{1}{4\sqrt{\pi}}\int_{\Lambda_{\rm cut}^{-2}}^{\infty}\frac{{\rm d}\,u}{u^{3/2}}\,\exp(-u\omega^2)\,. \qquad \text{(A.2)}$$

Appendix B. The pion-nucleon sigma-term $\sigma_{\pi N}$

The pion-nucleon sigma-term is an important quantity to learn about chiral symmetry breaking effects in the nucleon. The Feynman-Hellmann theorem [47] relates $\sigma_{\pi N}$ to the slope of $M_N(m)$ (with $m = m_q = m_u = m_d$ neglecting isospin breaking effects) as follows:

$$\sigma_{\pi N} \equiv m\,\frac{\partial M_N(m)}{\partial m} = m_\pi^2\,\frac{\partial M_N(m_\pi)}{\partial m_\pi^2}, \qquad \text{(B.1)}$$

where the second equality holds, strictly speaking, only for small m_π. Equation (B.1) offers a convenient way to learn about $\sigma_{\pi N}$ from lattice calculations of $M_N(m_\pi)$, see, *e.g.*, [22]. Direct lattice calculations are more difficult but possible, see, *e.g.*, [48].

Apart from (B.1) one also can evaluate in the model directly the actual definition of $\sigma_{\pi N}$ as double commutator of the strong interaction Hamiltonian with two axial isovector charges [49,50], or exploit a sum rule for the twist-3 distribution function $e(x)$ [51]. All three methods yield the same result in the χQSM [36].

By means of eq. (B.1) we obtain in the present study in the proper-time regularization: $\sigma_{\pi N} = 40\,$MeV. This agrees well with other χQSM calculations [30,49,50] performed in this regularization scheme.

In the χQSM the pion-nucleon sigma-term is quadratically UV-divergent, and as such particularly sensitive to details of regularization. In ref. [36] a way was found to compute $\sigma_{\pi N}$ in a regularization-scheme-independent way with the result $\sigma_{\pi N} \approx 68\,$MeV. The prize to pay for the regularization scheme independence was the use of an *approximation* expected to work within an accuracy of $\mathcal{O}(30\%)$ and well justified by notions from the instanton vacuum model.

On the basis of our results for $M_N(m_\pi)$ we are now in a position to check the accuracy of this approximation in practice. For that we note that the Feynman-Hellmann relation (B.1) allows to determine $M_N(m_\pi)$ from $\sigma_{\pi N}(m_\pi)$ up to an integration constant.

From the approximate (but regularization-scheme-independent) result for $\sigma_{\pi N}(m_\pi)$ from ref. [36] one obtains for $M_N(m_\pi)$ the result shown as dashed line in fig. 1, where for convenience the integration constant is chosen such that both curves coincide at a central value of $m_\pi = 1\,$GeV in the plot. We observe a good agreement of our exact result and the approximation of ref. [36], see fig. 1.

Also our result for $\sigma_{\pi N}$ agrees with the regularization-scheme-independent result for $\sigma_{\pi N}$ from ref. [36] to within the expected accuracy of $\mathcal{O}(30\%)$.

Thus, our results confirm that the instanton model motivated approximation advocated in [36] works well. Note, however, that here we went far beyond the study of ref. [36]. In this work we practically demonstrated that stable soliton solutions *do exist* also for large values of the pion mass, while in ref. [36] this was *presumed*.

The regularization-scheme-independent result of ref. [36] is in good agreement with recent extractions indicating $\sigma_{\pi N} = (60\text{–}70)\,$MeV [52], which is substantially more sizeable than the value obtained from earlier analyses [53].

In this context it is worthwhile mentioning that the spectrum of exotic ("pentaquark") baryons which were predicted in the framework of the χQSM [54] and for which recently possible observations were reported —see [55] for recent overviews— could provide an independent mean to access information on the pion-nucleon sigma-term [56]. The presently available data on the exotic baryons favour a large value for $\sigma_{\pi N}$ as found in [52].

Appendix C. Systematic uncertainty of the rotating soliton approach

The neglect of $\Delta = M_\Delta - M_N$ in the leading order of the large-N_c limit introduces a systematic uncertainty which is difficult to quantify. Here we roughly estimate this uncertainty on the basis of the soliton approach.

In this approach the nucleon and the Δ-resonance are just different rotational excitations of the same classic object, the soliton. A non-zero mass difference between the nucleon and the Δ-resonance arises due to considering a particular class of ("rotational") $1/N_c$ corrections [25,26]. The mass of an $SU(2)$-baryon M_B ($B = N$ or Δ in the real world with $N_c = 3$ colours) with spin S_B is given by

$$M_B = E_{\rm sol} + M_2 + S_B(S_B+1)\,\frac{\Delta}{3} + \cdots \qquad \text{(C.1)}$$

with $E_{\rm sol}$ as defined in eq. (9), M_2 denoting as in eq. (12) the $\mathcal{O}(N_c^0)$ correction to the baryon mass which is the same for the nucleon and the Δ-resonance, and the dots representing higher-order $1/N_c$ corrections.

Then, we obtain, as a first correction to M_N in eq. (22),

$$M_N(m_\pi, \Delta) = M_N(m_\pi, 0) + \frac{\Delta(m_\pi)}{4} + \ldots\,. \qquad \text{(C.2)}$$

Focusing on the linear-order correction in Δ and neglecting higher orders, we see that by neglecting Δ one underestimates the nucleon mass by about 70 MeV at the physical value of the pion mass. This is in good agreement with the systematic uncertainty roughly estimated in sect. 4.

References

1. K.G. Wilson, Phys. Rev. D **10**, 2445 (1974).
2. M. Creutz, *Quarks, Gluons and Lattices* (Cambridge University Press, Cambridge, 1983); C. Rebbi, *Lattice Gauge Theories and Monte Carlo Simulations* (World Scientific, Singapore, 1983).
3. CP-PACS Collaboration (S. Aoki *et al.*), Phys. Rev. D **60**, 114508 (1999) (arXiv:hep-lat/9902018); **67**, 034503 (2003) (arXiv:hep-lat/0206009).
4. CP-PACS Collaboration (A. Ali Khan *et al.*), Phys. Rev. D **65**, 054505 (2002); **67**, 059901(E) (2003).
5. JLQCD Collaboration (S. Aoki *et al.*), Phys. Rev. D **68**, 054502 (2003) (arXiv:hep-lat/0212039).
6. UKQCD Collaboration (C.R. Allton *et al.*), Phys. Rev. D **65**, 054502 (2002) (arXiv:hep-lat/0107021).
7. QCDSF-UKQCD Collaboration (A. Ali Khan *et al.*), Nucl. Phys. B **689**, 175 (2004) (arXiv:hep-lat/0312030).
8. Y. Aoki *et al.*, Phys. Rev. D **72**, 114505 (2005) (arXiv:hep-lat/0411006).
9. MILC Collaboration (C.W. Bernard *et al.*), Phys. Rev. D **64**, 054506 (2001) (arXiv:hep-lat/0104002).
10. MILC Collaboration (C. Aubin *et al.*), Phys. Rev. D **70**, 114501 (2004) (arXiv:hep-lat/0407028).
11. CSSM Lattice Collaboration (J.M. Zanotti *et al.*), Phys. Rev. D **65**, 074507 (2002) (arXiv:hep-lat/0110216).
12. J. Gasser, Ann. Phys. (N.Y.) **136**, 62 (1981).
13. J. Gasser, H. Leutwyler, Ann. Phys. (N.Y.) **158**, 142 (1984).
14. G. Colangelo, J. Gasser, H. Leutwyler, Nucl. Phys. B **603**, 125 (2001) (arXiv:hep-ph/0103088).
15. V. Bernard, T.R. Hemmert, U.G. Meissner, Nucl. Phys. A **732**, 149 (2004) (arXiv:hep-ph/0307115).
16. M. Procura, T.R. Hemmert, W. Weise, Phys. Rev. D **69**, 034505 (2004) (arXiv:hep-lat/0309020).
17. V. Bernard, T.R. Hemmert, U.G. Meissner, Phys. Lett. B **622**, 141 (2005) (arXiv:hep-lat/0503022).
18. M. Frink, U.G. Meissner, JHEP **0407**, 028 (2004) (arXiv:hep-lat/0404018); M. Frink, U.G. Meissner, I. Scheller, Eur. Phys. J. A **24**, 395 (2005) (arXiv:hep-lat/0501024).
19. S.R. Beane, Nucl. Phys. B **695**, 192 (2004) (arXiv:hep-lat/0403030).
20. D.B. Leinweber, D.H. Lu, A.W. Thomas, Phys. Rev. D **60**, 034014 (1999) (arXiv:hep-lat/9810005).
21. D.B. Leinweber, A.W. Thomas, K. Tsushima, S.V. Wright, Phys. Rev. D **61**, 074502 (2000) (arXiv:hep-lat/9906027).
22. D.B. Leinweber, A.W. Thomas, S.V. Wright, Phys. Lett. B **482**, 109 (2000) (arXiv:hep-lat/0001007).
23. R.D. Young, D.B. Leinweber, A.W. Thomas, S.V. Wright, Phys. Rev. D **66**, 094507 (2002) (arXiv:hep-lat/0205017).
24. D.B. Leinweber, A.W. Thomas, R.D. Young, Phys. Rev. Lett. **92**, 242002 (2004) (arXiv:hep-lat/0302020).
25. D.I. Diakonov, V.Y. Petrov, JETP Lett. **43**, 75 (1986) (Pisma Zh. Eksp. Teor. Fiz. **43**, 57 (1986)).
26. D.I. Diakonov, V.Y. Petrov, P.V. Pobylitsa, Nucl. Phys. B **306**, 809 (1988).
27. D.I. Diakonov, V.Y. Petrov, Nucl. Phys. B **245**, 259 (1984).
28. D.I. Diakonov, V.Y. Petrov, Nucl. Phys. B **272**, 457 (1986).
29. For reviews see, D.I. Diakonov, V.Y. Petrov, in *At the Frontier of Particle Physics*, edited by M. Shifman, Vol. **1** (World Scientific, Singapore, 2001) pp. 359-415 (arXiv:hep-ph/0009006); D. Diakonov, Prog. Part. Nucl. Phys. **51**, 173 (2003)(arXiv:hep-ph/0212026); arXiv:hep-ph/0406043.
30. D.I. Diakonov, V.Y. Petrov, M. Praszałowicz, Nucl. Phys. B **323**, 53 (1989).
31. C.V. Christov *et al.*, Prog. Part. Nucl. Phys. **37**, 91 (1996).
32. D.I. Diakonov *et al.*, Nucl. Phys. B **480**, 341 (1996); Phys. Rev. D **56**, 4069 (1997); K. Goeke, P.V. Pobylitsa, M.V. Polyakov, P. Schweitzer, D. Urbano, Acta Phys. Pol. B **32**, 1201 (2001); P. Schweitzer, D. Urbano, M.V. Polyakov, C. Weiss, P.V. Pobylitsa, K. Goeke, Phys. Rev. D **64**, 034013 (2001).
33. V.Y. Petrov, P.V. Pobylitsa, M.V. Polyakov, I. Börnig, K. Goeke, C. Weiss, Phys. Rev. D **57**, 4325 (1998); M. Penttinen, M.V. Polyakov, K. Goeke, Phys. Rev. D **62**, 014024 (2000); P. Schweitzer *et al.*, Phys. Rev. D **66**, 114004 (2002); **67**, 114022 (2003); Nucl. Phys. A **711**, 207 (2002); J. Ossmann, M.V. Polyakov, P. Schweitzer, D. Urbano, K. Goeke, Phys. Rev. D **71**, 034011 (2005) (arXiv:hep-ph/0411172).
34. R.F. Dashen, E. Jenkins, A.V. Manohar, Phys. Rev. D **49**, 4713 (1994); **51**, 2489(E) (1995).
35. C. Schüren, E. Ruiz Arriola, K. Goeke, Nucl. Phys. A **547**, 612 (1992).
36. P. Schweitzer, Phys. Rev. D **69**, 034003 (2004) (arXiv:hep-ph/0307336).
37. T.D. Cohen, W. Broniowski, Phys. Lett. B **292**, 5 (1992) (arXiv:hep-ph/9208253).
38. D.I. Diakonov, M.I. Eides, JETP Lett. **38**, 433 (1983) (Pisma Zh. Eksp. Teor. Fiz. **38**, 358 (1983)).
39. A. Dhar, R. Shankar, S.R. Wadia, Phys. Rev. D **31**, 3256 (1985).
40. E. Witten, Nucl. Phys. B **223**, 433 (1983).
41. P.V. Pobylitsa, E. Ruiz Arriola, T. Meissner, F. Grummer, K. Goeke, W. Broniowski, J. Phys. G **18**, 1455 (1992).
42. M. Gockeler *et al.*, in *Proceedings of Lattice 2005, 25-30 July 2005, Trinity College, Dublin*, hep-lat/0509196.
43. R. Sommer, Nucl. Phys. B **411**, 839 (1994) (arXiv:hep-lat/9310022).
44. K. Goeke, T. Ledwig, P. Schweitzer, A. Silva, in preparation.
45. ALPHA Collaboration (R. Sommer *et al.*), Nucl. Phys. Proc. Suppl. **129**, 405 (2004) (arXiv:hep-lat/0309171).
46. O. Bär, Nucl. Phys. Proc. Suppl. **140**, 106 (2005) (arXiv:hep-lat/0409123).
47. H. Hellmann, *Einführung in die Quantenchemie* (Leipzig, Deuticke Verlag, 1937); R.P. Feynman, Phys. Rev. **56**, 340 (1939).
48. S.J. Dong, J.F. Lagae, K.F. Liu, Phys. Rev. D **54**, 5496 (1996).
49. M. Wakamatsu, Phys. Rev. D **46**, 3762 (1992).
50. H.C. Kim, A. Blotz, C. Schneider, K. Goeke, Nucl. Phys. A **596**, 415 (1996).
51. P. Schweitzer, Phys. Rev. D **67**, 114010 (2003) (arXiv:hep-ph/0303011). For an overview on $e(x)$ see, A.V. Efremov, P. Schweitzer, JHEP **0308**, 006 (2003) (arXiv:hep-ph/0212044).
52. W.B. Kaufmann, G.E. Hite, Phys. Rev. C **60**, 055204 (1999); M.G. Olsson, Phys. Lett. B **482**, 50 (2000); M.M. Pavan, I.I. Strakovsky, R.L. Workman, R.A. Arndt, πN

Newslett. **16**, 110 (2002) (arXiv: hep-ph/0111066); M.G. Olsson, W.B. Kaufmann, πN Newslett. **16**, 382 (2002).
53. R. Koch, Z. Phys. C **15**, 161 (1982); J. Gasser, H. Leutwyler, M. E. Sainio, Phys. Lett. B **253**, 252; 260 (1991).
54. D.I. Diakonov, V.Y. Petrov, M.V. Polyakov, Z. Phys. A **359**, 305 (1997) (arXiv:hep-ph/9703373).
55. K. Hicks, arXiv:hep-ex/0412048; T. Nakano, Nucl. Phys. A **738**, 182 (2004).
56. P. Schweitzer, Eur. Phys. J. A **22**, 89 (2004) (arXiv:hep-ph/0312376).